ACS Catalysis

Research Article

Cite This: ACS Catal. 2019, 9, 11067−11073

pubs.acs.org/acscatalysis

Vanadium-Catalyzed Selective Oxidative Homocoupling of Alkenyl Phenols To Synthesize Lignan Analogs

William C. Neuhaus, Adriana L. Jemison, and Marisa C. Kozlowski*

Department of Chemistry, Roy and Diana Vagelos Laboratories, University of Pennsylvania, Philadelphia, Pennsylvania 19104, United States

Supporting Information

ABSTRACT: The oxidative homocoupling of *para*-alkenyl phenols and subsequent trapping of the resulting quinone methide with a variety of oxygen and nitrogen nucleophiles were achieved. Both *β*-*β* and *β*-O coupling isomers can be synthesized via either C−C coupling and two nucleophilic additions of one water molecule (*β*-*β* isomer) or C−O coupling followed by one nucleophilic addition of a water molecule (*β*-O isomer), respectively. Selectivity between these outcomes was achieved by leveraging the understanding of the mechanism. Specifically, a qualitative predictive model for the selectivity of the coupling was formulated based on catalyst electronics, solvent polarity, and concentration.

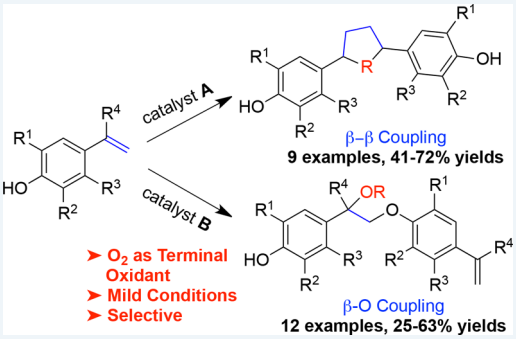

KEYWORDS: *vanadium, lignans, biomimetic, phenol oxidation, oxidative coupling, tetrahydrofurans*

Downloaded via UNIV OF PENNSYLVANIA on January 7, 2020 at 15:32:13 (UTC).
See https://pubs.acs.org/sharingguidelines for options on how to legitimately share published articles.

INTRODUCTION

Lignans are a class of molecules found abundantly in nature (Figure 1). Some natural products in this class have been found to possess potent biological activities including antimalarial,[1] antioxidant, antiparasitic, antifungal,[2] and antimicrobial properties.[3] The tetrahydrofuranyl scaffold lignans have potent activity against *Trypanosoma cruzi*, the causative agent of Chagas disease,[4] as well as being highly active platelet-activating factor (PAF) inhibitors.[5]

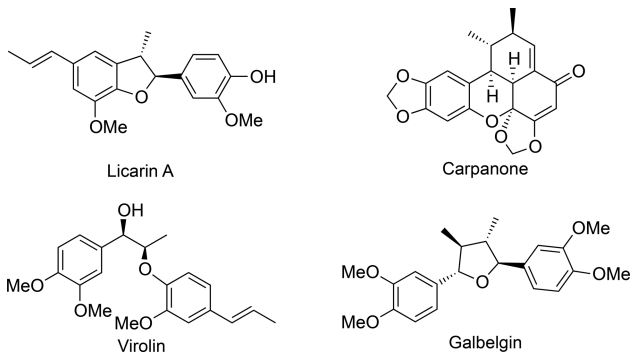

Figure 1. Examples of alkenyl phenol homocoupling products found in nature.

Vanadium(V) oxo catalysts have been used to selectively and enantioselectively homocouple hydroxy aryl systems, such as phenols, naphthols, and hydroxycarbazoles.[6−10] We hypothesized that alkenyl phenols should also be oxidizable by this class of vanadium catalysts. These catalysts have the advantage of being able to be turned over by molecular oxygen and are relatively inexpensive to prepare compared to precious metal catalysts.

To the best of our knowledge, no general method exists to catalytically and oxidatively homocouple terminal alkenyl phenols selectively. In 1997, it was reported that *para*-methoxy styrene could be homocoupled to give the quinone intermediate that was trapped with water to form a diaryl furan (*β*-*β* coupling) in modest yields using ceric ammonium nitrate (CAN) (Scheme 1.1).[11] In 2011, the oxidative enzyme laccase was studied with a simple styrene and was found to give a variety of oxidation products, including tetrahydrofuranyl and aryl ether scaffolds of interest, as a low yielding mixture (Scheme 1.2).[12] In 2015, a method was reported to generate the aryl ether linkage (*β*-O coupling) seen in virolin. This method lacked generalizability and required stoichiometric silver as an oxidant (Scheme 1.3).[13] While other methods to synthesize tetrahydrofuranyl lignans have been reported, none follow a biomimetic oxidative homocoupling route.[14,15]

RESULTS AND DISCUSSION

En route to synthesizing a carpanone[16,17] analog utilizing a vanadium(V) catalyst, we discovered that a tetrahydrofuran product was formed instead (Scheme 2). Based on this outcome, 10 equiv of water were added to the reaction mixture in order to facilitate the formation of the tetrahydrofuran product. This strategy proved effective, resulting in a 46% yield

Received: June 20, 2019
Revised: September 12, 2019
Published: October 23, 2019

© 2019 American Chemical Society

DOI: 10.1021/acscatal.9b02608
ACS Catal. 2019, 9, 11067−11073

Scheme 1. Styrene and Styrenyl Phenol Oxidative Coupling To Affect β-β coupling and β-O Coupling

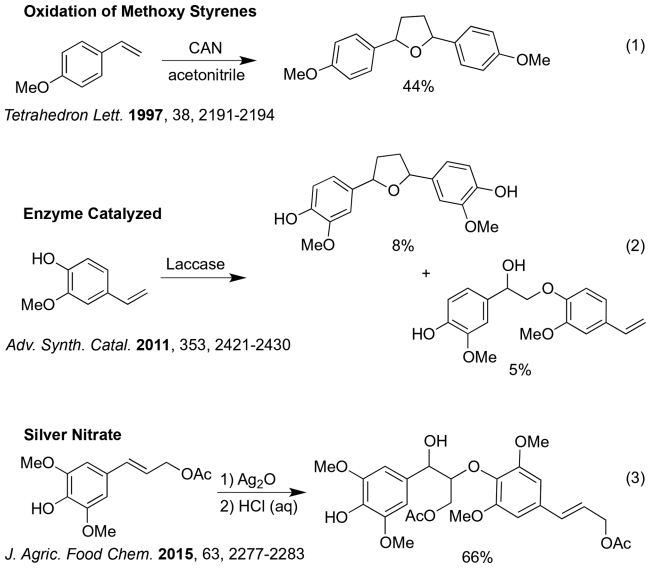

Scheme 2. Discovery Reaction

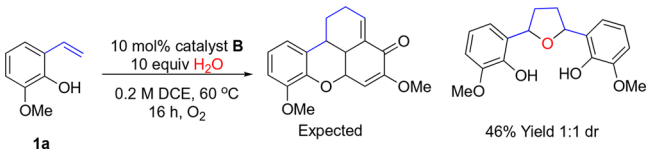

of product as a mixture of *cis* and *trans* tetrahydrofuranyl isomers.

Curious as to whether *para*-alkenyl phenol substrates would react similarly, these substrates were also investigated. Notably, two avenues were observed arising from either C−C coupling and two nucleophilic additions of one water molecule (β-β isomer) or C−O coupling followed by one nucleophilic addition of a water molecule (β-O isomer). With a substrate, **1b**, which gives both β-β and the β-O coupling isomers in relatively high yield, solvent screening revealed a strong correlation between the ratio of the coupling products and the dipole moment of reaction solvent (Scheme 3). Using these data, conditions were devised that led to selectivity for either the β-β or β-O coupling products. Optimal results for the β-β coupling product were obtained in acetonitrile, while 1,4-dioxane was best to generate the β-O coupling products.

Further screening was undertaken with catalysts having different electronic and structural properties (Figure 2). The yield and selectivity (Table 1) were not sensitive to the properties of the monomeric catalysts. However, the dimeric catalyst **B** gave a 5.8:1 selectivity in favor of the β-O product (Table 1, entry 2). This outcome could arise from either a synergistic effect between the two vanadium centers or the effectively higher concentration of vanadium centers/catalytic sites in solution. Base additives seemed to suppress the desired reactivity (Table 1, entries 6−9).

From these observations, it appears that the concentrations of both the catalytic species and substrate impact the selectivity. It was hypothesized that dilution of the reaction mixture would therefore result in different selectivity ratios by biasing pathways with lower molecularity (Figure 3). Two parallel sets of experiments were performed in acetonitrile and

Scheme 3. Optimization of Selectivity by High-Throughput Experimentation[a]

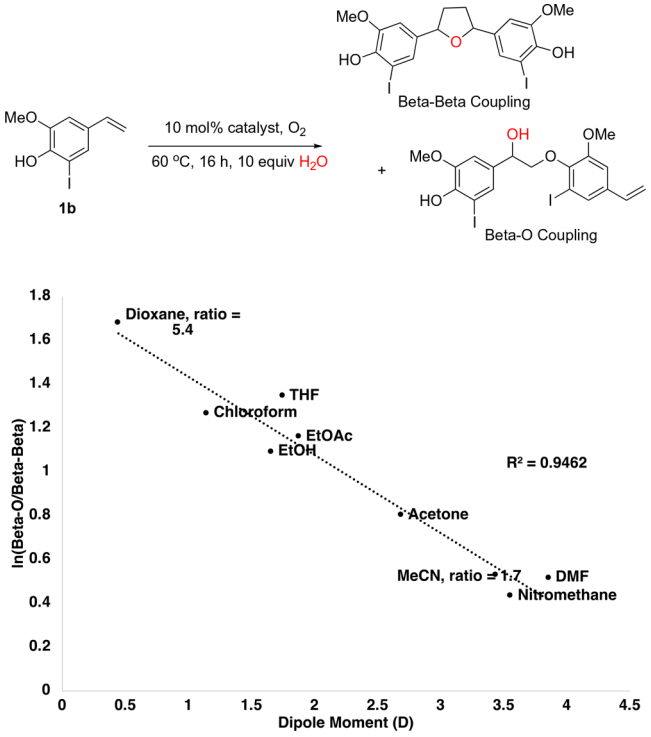

[a]Ratios are of peak areas from ultra-performance liquid chromatography (UPLC) analysis of the reaction mixture using UV−vis detection using total wavelength chromatogram (TWC).

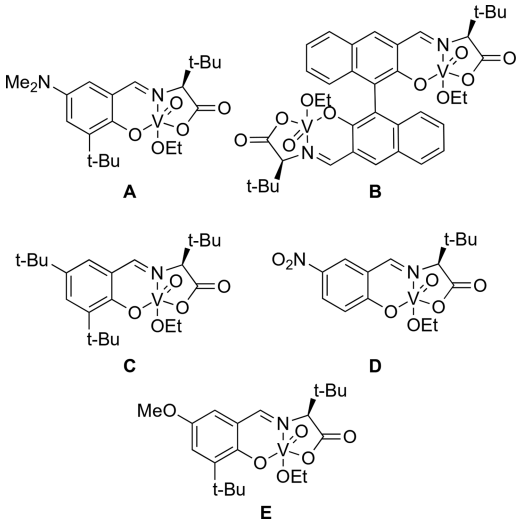

Figure 2. Catalysts screened for selectivity.

1,4-dioxane, as these were found to give the best results for each isomer. For the trials in 1,4-dioxane, it was found that a linear relationship existed between the selectivity ratio and the starting concentration of the phenol. At very low concentrations in 1,4-dioxane, only decomposition was observed. In acetonitrile, the selectivity followed a more logarithmic trend. In both cases, lower concentrations resulted in more β-β coupling products, while higher concentrations gave more β-O coupling products.

A double reciprocal analysis of the selectivity versus the global concentration in acetonitrile showed a linear trend with

DOI: 10.1021/acscatal.9b02608
ACS Catal. 2019, 9, 11067−11073

Table 1. Ratio of Products from Screening of Catalysts and Additives[a]

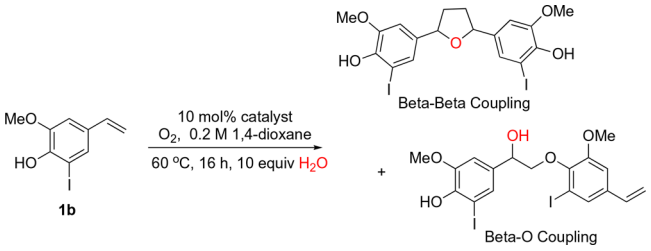

entry	additive	catalyst	% β-β[a]	% β-O[a]	β-O/β-β
1	none	**A**	28	68	2.4
2	none	**B**	12	70	5.8
3	none	**C**	19	73	3.8
4	none	**D**	22	66	3.0
5	none	**E**	14	49	3.5
6	$NaHCO_3$	**A**	18	12	2.8
7	Na_2CO_3	**A**	0	0	N/A
8	KOH	**A**	0	0	N/A
9	K_2CO_3	**A**	0	0	N/A

[a]Yields determined by ^{1}H NMR spectroscopy of the reaction mixture with CH_2Br_2 as an internal standard.

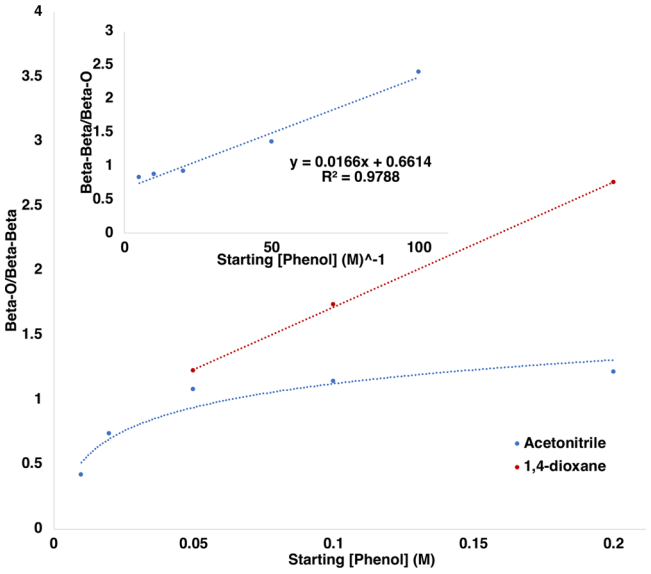

Figure 3. Dilution effects on selectivity. (Yields determined by ^{1}H NMR spectroscopy of the reaction mixture with CH_2Br_2 as an internal standard. Reaction conditions: 10 mol % catalyst **A**, 16 h, 10 equiv water, and 80 °C.)

excellent correlation (R^2 = 0.98) (Figure 3, inset). This result indicated that, at high concentrations of the substrate in acetonitrile, the catalyst was being saturated by the substrate, while at low concentrations, not all of the catalytic sites were being used.

On this basis, catalyst loading was expected to have an effect on selectivity. Indeed, in both 1,4-dioxane and acetonitrile, there were strong linear relationships between the catalyst loading and selectivity (Figure 4). In both solvents, the amount of the β-O product increased with catalyst loading relative to the β-β product. It is reasonable to conclude that a metal-bound pathway contributes more to the production of the β-O coupling product than the β-β coupling product.

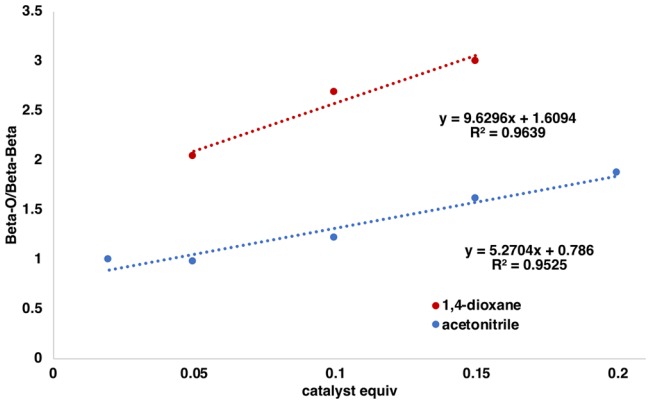

Figure 4. Catalyst loading effect on selectivity. (Yields determined by ^{1}H NMR spectroscopy of the reaction mixture with CH_2Br_2 as an internal standard. Reaction conditions: *x* mol % catalyst **A**, 16 h, 10 equiv water, 0.2 M substrate, and 80 °C.)

To better understand these observations, a series of experiments were performed to measure selectivity while changing the concentration of phenol and holding the concentration of catalyst constant (Figure 5). From the

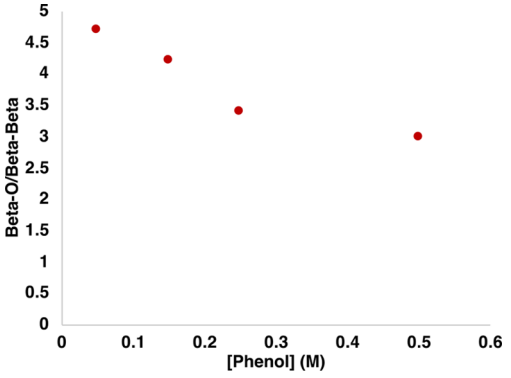

Figure 5. [Phenol] versus selectivity in 1,4-dioxane. (Ratios are of peak areas from UPLC analysis of the reaction mixture using UV−vis detection with TWC. Reaction conditions: 0.724 mL of dioxane, 0.01 M catalyst **A**, 16 h, 1 M H_2O, and 80 °C.)

above observations, it was expected that higher concentrations of phenol would lead to more β-β products relative to the β-O coupling product. Indeed, this trend was observed and, in conjunction with previous results, indicated that free phenol could be displacing bound oxidized phenol, allowing free phenoxy radicals to couple in an uncatalyzed fashion to generate the β-β coupling product.

With this understanding, conditions could be rationally designed that would produce the β-β coupling product selectively (Table 2). The catalyst library was screened, and again the ratio of isomers was insensitive to catalyst electronics. However, the electron-rich dimethylamino-substituted catalyst (catalyst **A**) gave fewer byproducts. This observation can be explained by the strong electron-donating groups on the ligand, which stabilize the high oxidation state of the metal, making the catalyst a milder oxidant relative to other variants. The reaction mixture was diluted as much as was operationally reasonable to minimize the coupling of a catalyst-bound intermediate and maximize the coupling of free phenoxy radicals. At a very dilute (0.005 M) concentration in

DOI: 10.1021/acscatal.9b02608
ACS Catal. 2019, 9, 11067−11073

Table 2. Optimization of *β-β* Coupling[a]

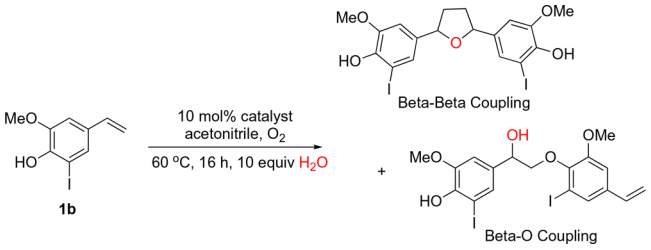

entry	[Phenol] (M)	catalyst	% *β-β*	% *β*-O	*β*-O/*β-β*
1	0.2	**A**	40	46	1.2
2	0.2	**B**	39	43	1.1
3	0.2	**C**	32	38	1.2
4	0.2	**D**	26	28	1.1
5	0.2	**E**	39	34	0.87
6	0.01	**A**	43	25	0.58
7	0.005	**A**	65	16	0.25

[a]Yields determined by ^{1}H NMR spectroscopy of the reaction mixture with CH_2Br_2 as an internal standard.

acetonitrile, moderate yields of the *β-β* coupling product were obtained with a 1:4 (*β*-O/*β-β*) selectivity.

Several common oxidants other than oxygen were tested to ensure that a stronger oxidant was not needed to achieve higher yields. Substrate **1b** was subjected to the conditions optimized for *β-β* coupling, and the reaction mixture was measured by ^{1}H NMR spectroscopy using an added internal standard. All four oxidants tested gave poorer performance and selectivity than with oxygen as the terminal oxidant for substrate **1d** (Table 3). This result likely arises from direct over-oxidation of the product by other oxidants.

Table 3. ^{1}H NMR Yield for *β-β* and *β*-O Coupling Products Using Four Chemical Oxidants

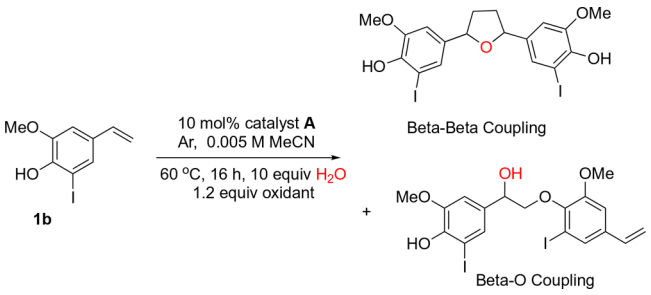

entry	oxidant	% **1b**[a]	% *β*-O coupling[a]	% *β-β* coupling[a]
1	*tert*-butyl hydroperoxide (70% in H_2O)	trace	28	28
2	$(NH_4)_2S_2O_8$	10	12	trace
3	iodosobenzene	10	12	52
4	H_2O_2 (30% in H_2O)	30	20	32

[a]Yields determined by ^{1}H NMR spectroscopy of the reaction mixture with CH_2Br_2 as internal standard.

Seeing that control of selectivity could be achieved by selection of solvent, catalyst, and concentration, the mechanism was probed using 2,2,6,6-tetramethylpiperidine 1-oxyl (TEMPO) as a free radical trap. Two equivalents of TEMPO were added to the optimized *β-β* coupling conditions, and TEMPO-trapped products were isolated (see the Supporting Information for experimental details and characterization data). This result indicates that free radical intermediates persist in solution (Scheme 4, intermediate **4**). The major

Scheme 4. Proposed Mechanism for Oxidative Coupling of *para*-Alkenyl Phenols

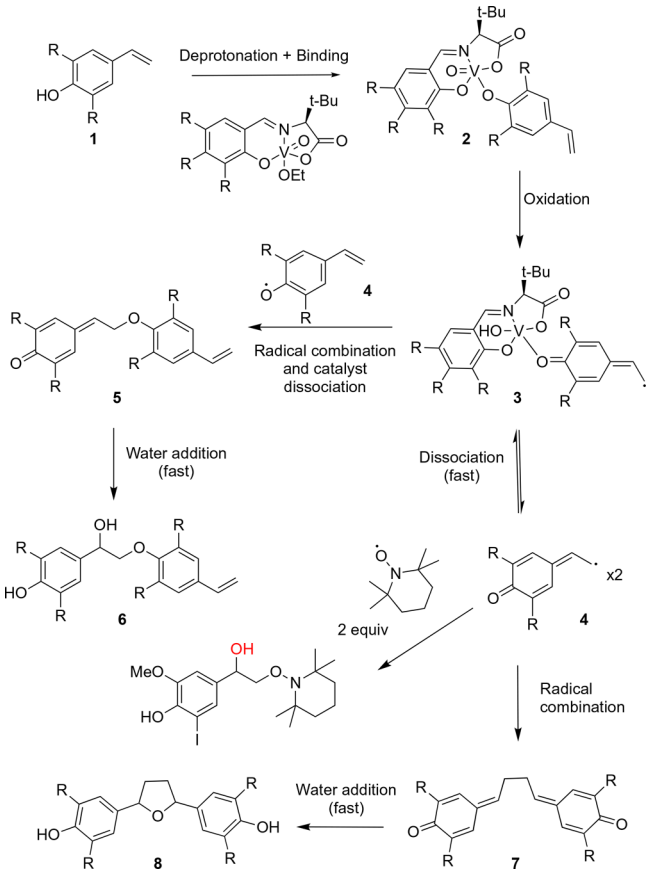

product was not the expected *β-β* coupling product as predicted for these conditions in the absence of TEMPO. It appears that sequestering free phenoxy radicals drove the reaction toward the *β*-O coupling product through a catalyst-bound intermediate that interacts less readily with TEMPO.

From the above data, the following mechanism is proposed (Scheme 4). First, free phenol undergoes ligand exchange with the catalyst and is oxidized to form intermediate **3**. Binding of the phenol oxygen to the catalyst should be facile given the known Lewis acidity of vanadium(V) oxo catalysts.[18] Evidence for coordination of the substrates was obtained with ^{51}V NMR spectroscopy (see the Supporting Information for details). Electron-rich phenols shift the ^{51}V signal more significantly than electron-poor phenols. Mixing catalyst **A** or **B** with electron-rich 2-fluoro-6-methoxy-4-vinyl phenol (**1h**) or 2,6-dimethoxy-4-vinyl phenol (**1j**) substrates results in a quick loss of the catalyst ^{51}V signal and the appearance of a new signal downfield. In the case of the 2-iodo-6-methoxy4-vinyl phenol (**1b**) with catalyst **B**, the catalyst signal decreases and a smaller peak appears over several hours. The ^{51}V signal is shifted further downfield the more electron-rich the ligand, as expected for complexes of vanadium(V).[20,21] On the other hand, 2-methoxy-6-nitro-4-vinyl phenol (**1i**) does not affect the vanadium chemical shift of either catalyst, indicating a very weak or disfavorable coordination. These results together indicate that electron-rich phenols interact more readily with

DOI: 10.1021/acscatal.9b02608
ACS Catal. 2019, 9, 11067−11073

the catalysts than electron-poor phenols, which is consistent with the observed reaction profiles (slower reactions for electron-poor substrates; see below).

The reaction undergoes a single turnover when conducted under nitrogen, indicating that the vanadium(V) species can act on the substrate without oxygen. The resultant intermediate **3** is biased to attack by the phenolic oxygen of unbound **4** to form the aryl ether bond giving intermediate **5** and, after addition of water, the β-O coupling product **6**. Coupling to form the C−O bond is preferred in this case because the Lewis acidic vanadium polarizes the bound substrate, rendering the β-position harder and thus more susceptible to attack by oxygen instead of carbon. This result is consistent with the finding of more C−O at higher concentrations of the vanadium catalyst (allows sufficient **3** to be present; see Scheme 4). Alternatively, the oxidized free radical species **4** could homocouple, leading to the β-β coupling product **8**, after addition of water. Dissociation from the catalyst is more likely in more polar solvents such as acetonitrile due to stabilization of the resulting cationic vanadium species such that less **3** is present, favoring C−C coupling and disfavoring C−O coupling. Coupling to form the C−C bond from the unbound phenolic radical is favored due to greater density of the SOMO (singly occupied molecular orbital) at the β-carbon (see the Supporting Information) and less steric hindrance at the β-carbon versus the oxygen. This sequence is consistent with the mechanism proposed for an enzyme-catalyzed oxidative homocoupling of coniferyl alcohol.[19]

The substrate scope was explored for both the β-O coupling and the β-β coupling. For the β-O coupling (Scheme 5) scope, modestly electron-poor alkenyl phenols gave the best results. Very electron-poor alkenyl phenols, like the nitro-substituted **1i,** react more slowly, requiring elevated reaction temperatures and leaving the unreacted starting material. More electron-rich substrates are active but do not convert to the desired products under these conditions; instead, a complex reaction mixture results. These observations are consistent with the hypothesized mechanism. Electron-poor phenols are harder to oxidize and require harsher conditions, while more electron-rich phenols are more readily oxidized and may have a tendency to over-oxidize or decompose under the reaction conditions.

Unfortunately, phenols that are unsubstituted at one *ortho* position do not give a significant amount of the β-O product. Yields for the β-O coupled products are moderate, partially due to the instability of the product and difficult purification from related byproducts. However, no method has been reported for this coupling across such a range of substrates. Scaling up the reaction did impact the yield (Scheme 5, **6b**). Substituted alkenes gave poorer yields (Scheme 5, **6f**) compared to the unsubstituted counterparts, potentially due to greater steric hindrance toward the attack by the phenoxy radical (Scheme 4, **3** to **5**) or water (Scheme 4, **5** and **6**).

Since water acts as the nucleophile to trap intermediate quinone methide **5** (Scheme 4), other nucleophiles were examined (Scheme 6). Addition of alcohol nucleophiles was effective using 1,2-dichloroethane as the solvent (to more readily exclude water) using the highest yielding substrate (**1b**) and the optimal conditions for β-O coupling.

The scope for the β-β coupling is more general and tolerates both electron-rich and electron-poor alkenyl phenol substrates (Scheme 7). Apparently, the low concentration of the reaction mixture reduces undesired side reactions, and the tetrahydrofuranyl scaffold is more stable overall. The yields are moderate to good with 1.2−1.8:1 of the *cis*:*trans* tetrahydrofuran isomers. The yield and selectivity are not significantly impacted by the scale of the reaction (Scheme 7, **8j**). In some cases, isolated yields are limited by the difficulty of purifying the product from isomers or decomposed species. The β-β and β-O reactions with water and aniline are especially affected, but reactions with alcohols are much easier to separate as the ether products (**9d**) have significantly different behaviors on silica

Scheme 5. Scope of the β-O Coupling

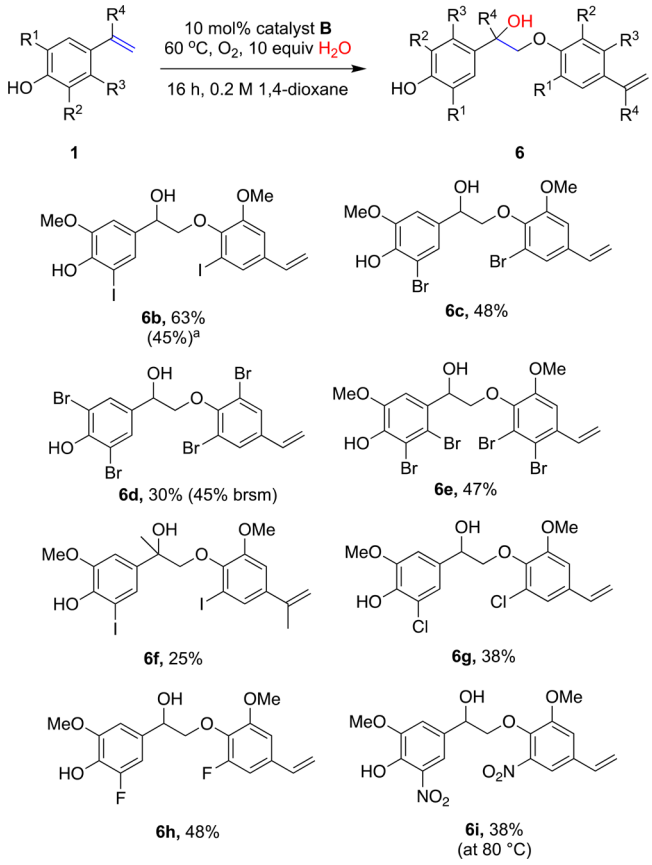

[a]Reaction at a 1 mmol scale.

Scheme 6. Scope of the β-O Coupling with Alcohol Nucleophiles

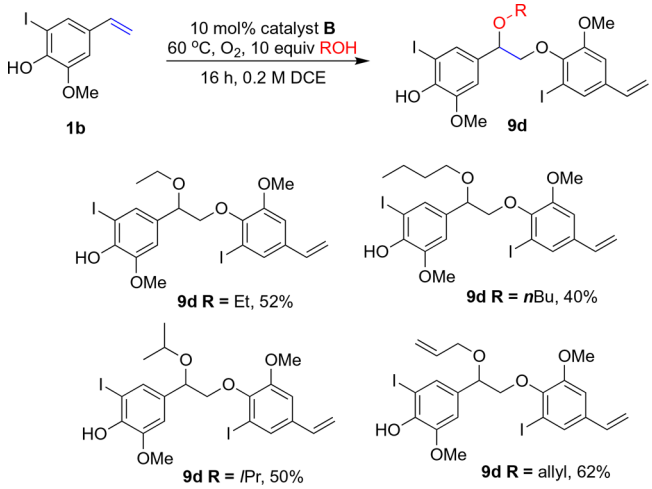

DOI: 10.1021/acscatal.9b02608
ACS Catal. 2019, 9, 11067−11073

Scheme 7. Scope of the *β-β* Coupling[a]

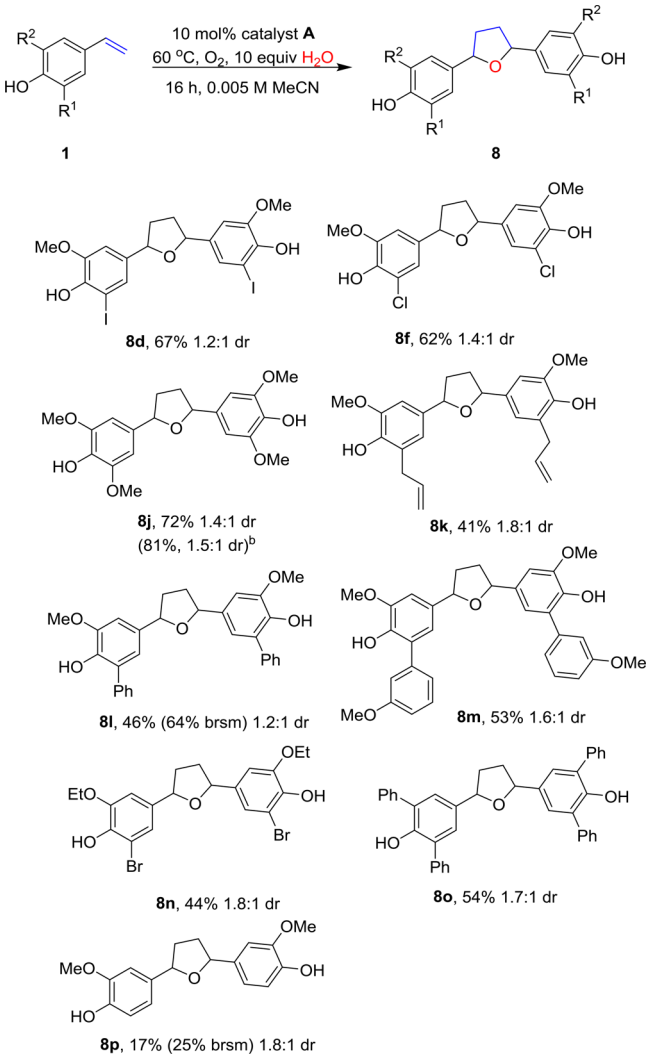

[a]Diastereomeric ratios of *trans*:*cis* were determined from comparison with ^{1}H NMR spectra of analogous tetrahydrofurans.[22] [b]1 mmol scale.

gel. Both mono and bis *ortho*-substituted phenols tolerated these reaction conditions; however a poor yield was seen for the mono-substituted example (Scheme 7, **8p**), most likely due to a greater number of possible byproducts.

After exploring the scope of the *β-β* coupling, nucleophiles other than water were investigated as trapping agents for the intermediate quinone methide **7** (Scheme 4). Aniline was found to be an effective nucleophile in the *β-β* coupling (Scheme 8). Higher concentrations of the substrate were needed to accelerate the reaction and prevent decomposition of the aniline nucleophile.

Scheme 8. *β-β* Coupling with Aniline as the Nucleophile

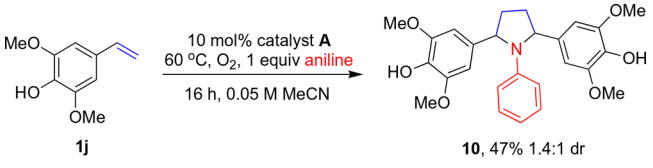

In conclusion, mechanistic experiments and strategic high-throughput experimentation were investigated to rationally optimize reaction conditions and bias the outcome of the oxidative coupling of alkenyl phenols. The result is a general method to generate tetrahydrofuranyl lignan derivatives via a biomimetic coupling mechanism. We also report the synthesis of several aryl ether coupling products, which, to our knowledge, have no known catalytic synthesis. The products resulting from both methods can be further diversified by using either alcohol or aniline nucleophiles. Complex structures can be synthesized selectively in one step to afford multiple products from one substrate. These structures have potential biological relevance due to their similarities to common natural products. The use of molecular oxygen as an environmentally benign terminal oxidant and the relatively low toxicity of vanadium minimize the impact of waste streams.

■ ASSOCIATED CONTENT

Supporting Information

The Supporting Information is available free of charge on the ACS Publications website at DOI: 10.1021/acscatal.9b02608.

Experimental procedures for all experiments and characterization data (PDF)

■ AUTHOR INFORMATION

Corresponding Author

*E-mail: marisa@sas.upenn.edu.

ORCID

Adriana L. Jemison: 0000-0003-2705-7181

Marisa C. Kozlowski: 0000-0002-4225-7125

Notes

The authors declare no competing financial interest.

■ ACKNOWLEDGMENTS

We are grateful to the NSF (CHE1764298) and the NIH (R35 GM131902 and RO1 GM112684) for financial support of this research. Partial instrumentation support was provided by the NIH and NSF (1S10RR023444, 1S10RR022442, CHE-0840438, CHE-0848460, 1S10OD011980, and CHE-1827457). Dr. Charles W. Ross III is acknowledged for obtaining accurate mass data.

■ REFERENCES

(1) Zhang, H.-J.; Tamez, P. A.; Hoang, V. D.; Tan, G. T.; Hung, N. V.; Xuan, L. T.; Huong, L. M.; Cuong, N. M.; Thao, D. T.; Soejarto, D. D.; Fong, H. H. S.; Pezzuto, J. M. Antimalarial Compounds from Rhaphidophora decursiva. *J. Nat. Prod.* **2001**, *64*, 772−777.

(2) Rye, C. E.; Barker, D. Asymmetric Synthesis and Anti-protozoal Activity of the 8,4′-oxyneolignans Virolin, Surinamensin and Analogues. *Eur. J. Med. Chem.* **2013**, *60*, 240−248.

(3) Teponno, R. B.; Kusari, S.; Spiteller, M. Recent Advances in Research on Lignans and Neolignans. *Nat. Prod. Rep.* **2016**, *33*, 1044−1092.

(4) Hartmann, A. P.; de Carvalho, M. R.; Bernardes, L. S. C.; Moraes, M. H. d.; de Melo, E. B.; Lopes, C. D.; Steindel, M.; da Silva, J. S.; Carvalho, I. Synthesis and 2D-QSAR Studies of Neolignan-based Diaryl-tetrahydrofuran and -Furan Analogues with Remarkable Activity Against Trypanosoma cruzi and Assessment of the Trypanothione Reductase Activity. *Eur. J. Med. Chem.* **2017**, *140*, 187−199.

(5) Jung, K. Y.; Kim, D. S.; Oh, S. R.; Park, S.-H.; Lee, I. S.; Lee, J. J.; Shin, D.-H.; Lee, H.-K. Magnone A and B, Novel Anti-PAF

DOI: 10.1021/acscatal.9b02608
ACS Catal. 2019, 9, 11067−11073

Tetrahydrofuran Lignans from the Flower Buds of Magnolia fargesii. *J. Nat. Prod.* **1998**, *61*, 808−811.
(6) Liu, L.; Carroll, P. J.; Kozlowski, M. C. Vanadium-Catalyzed Regioselective Oxidative Coupling of 2-Hydroxycarbazoles. *Org. Lett.* **2015**, *17*, 508−511.
(7) Kang, H.; Herling, M. R.; Niederer, K. A.; Lee, Y. E.; Vasu Govardhana Reddy, P.; Dey, S.; Allen, S. E.; Sung, P.; Hewitt, K.; Torruellas, C.; Kim, G. J.; Kozlowski, M. C. Enantioselective Vanadium-Catalyzed Oxidative Coupling: Development and Mechanistic Insights. *J. Org. Chem.* **2018**, *83*, 14362−14384.
(8) Kim, H. Y.; Takizawa, S.; Sasai, H.; Oh, K. Reversal of Enantioselectivity Approach to BINOLs via Single and Dual 2-Naphthol Activation Modes. *Org. Lett.* **2017**, *19*, 3867−3870.
(9) Hwang, D.-R.; Chen, C.-P.; Uang, B.-J. Aerobic Catalytic Oxidative Coupling of 2-naphthols and Phenols by $VO(acac)_2$. *Chem. Commun.* **1999**, 1207−1208.
(10) Luo, Z.; Liu, Q.; Gong, L.; Cui, X.; Mi, A.; Jiang, Y. The Rational Design of Novel Chiral Oxovanadium(iv) Complexes for Highly Enantioselective Oxidative Coupling of 2-naphthols. *Chem. Commun.* **2002**, 914−915.
(11) Nair, V.; Mathew, J.; Kanakamma, P. P.; Panicker, S. B.; Sheeba, V.; Zeena, S.; Eigendorf, G. K. Novel Cerium(IV) Ammonium Nitrate Induced Dimerization of Methoxystyrenes. *Tetrahedron Lett.* **1997**, *38*, 2191−2194.
(12) Gavezzotti, P.; Navarra, C.; Caufin, S.; Danieli, B.; Magrone, P.; Monti, D.; Riva, S. Synthesis of Enantiomerically Enriched Dimers of Vinylphenols by Tandem Action of Laccases and Lipases. *Adv. Synth. Catal.* **2011**, *353*, 2421−2430.
(13) Kishimoto, T.; Takahashi, N.; Hamada, M.; Nakajima, N. Biomimetic Oxidative Coupling of Sinapyl Acetate by Silver Oxide: Preferential Formation of β-O-4 Type Structures. *J. Agric. Food Chem.* **2015**, *63*, 2277−2283.
(14) Jagtap, P. R.; Císařová, I.; Jahn, U. Bioinspired Total Synthesis of Tetrahydrofuran Lignans by Tandem Nucleophilic Addition/redox Isomerization/oxidative Coupling and Cycloetherification Reactions as Key Steps. *Org. Biomol. Chem.* **2018**, *16*, 750−755.
(15) Albertson, A. K. F.; Lumb, J.-P. A Bio-Inspired Total Synthesis of Tetrahydrofuran Lignans. *Angew. Chem., Int. Ed.* **2015**, *54*, 2204−2208.
(16) Liron, F.; Fontana, F.; Zirimwabagabo, J.-O.; Prestat, G.; Rajabi, J.; Rosa, C. L.; Poli, G. A New Cross-Coupling-Based Synthesis of Carpanone. *Org. Lett.* **2009**, *11*, 4378−4381.
(17) Chapman, O. L.; Engel, M. R.; Springer, J. P.; Clardy, J. C. Total Synthesis of Carpanone. *J. Am. Chem. Soc.* **1971**, *93*, 6696−6698.
(18) Rana, S.; Haque, R.; Santosh, G.; Maiti, D. Decarbonylative Halogenation by a Vanadium Complex. *Inorg. Chem.* **2013**, *52*, 2927−2932.
(19) Davin, L. B.; Lewis, N. G. Dirigent Phenoxy Radical Coupling: Advances and Challenges. *Curr. Opin. Biotechnol.* **2005**, *16*, 398−406.
(20) Cornman, C. R.; Colpas, G. J.; Hoeschele, J. D.; Kampf, J.; Pecoraro, V. L. Implications for the Spectroscopic Assignment of Vanadium Biomolecules: Structural and Spectroscopic Characterization of Monooxovanadium(V) Complexes Containing Catecholate and Hydroximate Based Noninnocent ligands. *J. Am. Chem. Soc.* **1992**, *114*, 9925−9933.
(21) Priebsch, W.; Rehder, D. Preparation and vanadium-51 NMR Characteristics of Oxovanadium(V) Compounds. Relation Between Metal Shielding and Ligand Electronegativity. *Inorg. Chem.* **1985**, *24*, 3058−3062.
(22) Imada, Y.; Okada, Y.; Noguchi, K.; Chiba, K. Selective Functionalization of Styrenes with Oxygen Using Different Electrode Materials: Olefin Cleavage and Synthesis of Tetrahydrofuran Derivatives. *Angew. Chem., Int. Ed.* **2019**, *58*, 125−129.

DOI: 10.1021/acscatal.9b02608
ACS Catal. 2019, 9, 11067−11073